Electronic Supplementary Material (ESI) for Journal of Materials Chemistry A.
This journal is © The Royal Society of Chemistry 2022

Supporting Information

Expansion force induced *in-situ* formation of 3D boron nitride network for light-weight, low-k, low-loss, and thermally conductive composites

Shiqing Zhou, [a,b] Yanting Xu, [a] Jiayue Tang, [a] Kaijing Qian, [a] Jun Zhao, [a] Jun Wang, [a] Hongwen Gao, [b] Zhuo Li * [a]

[a] *Department of Materials Science, Fudan University,220 Handan Road, Shanghai 200433, P. R. China*

[b] *College of Environmental Science and Engineering, Tongji University1239, Siping Road, Shanghai 200092, P. R. China*

*Corresponding author. E-mail: zhuo_li@fudan.edu.cn

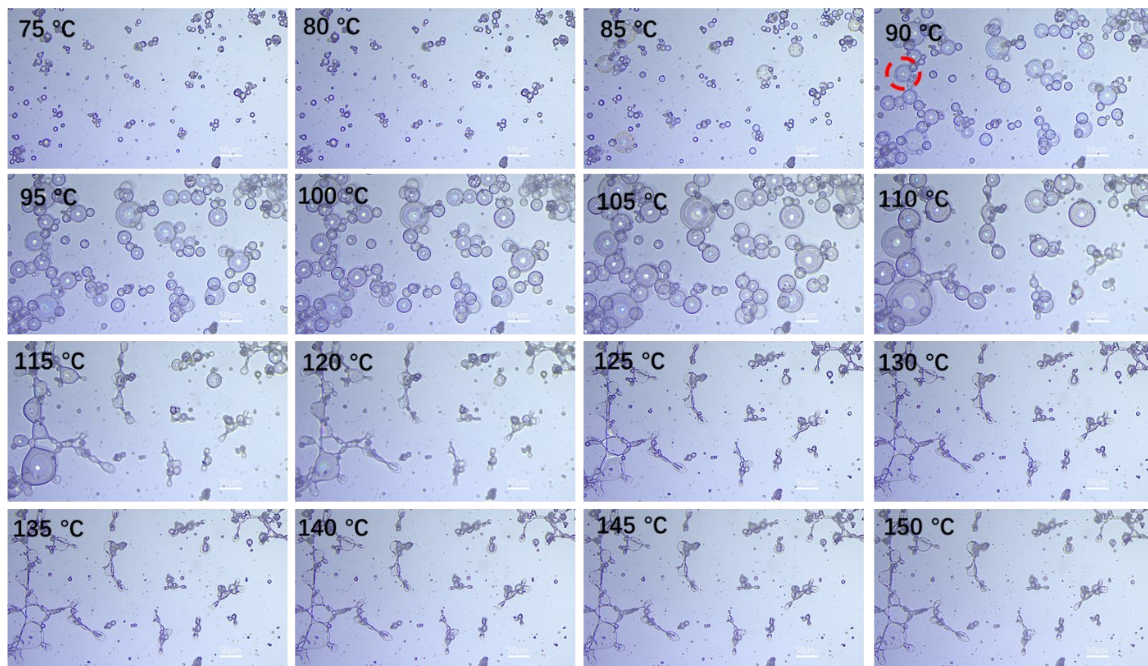

Figure S1. Microscopic images of EMs at different temperatures (75 °C -150 °C).

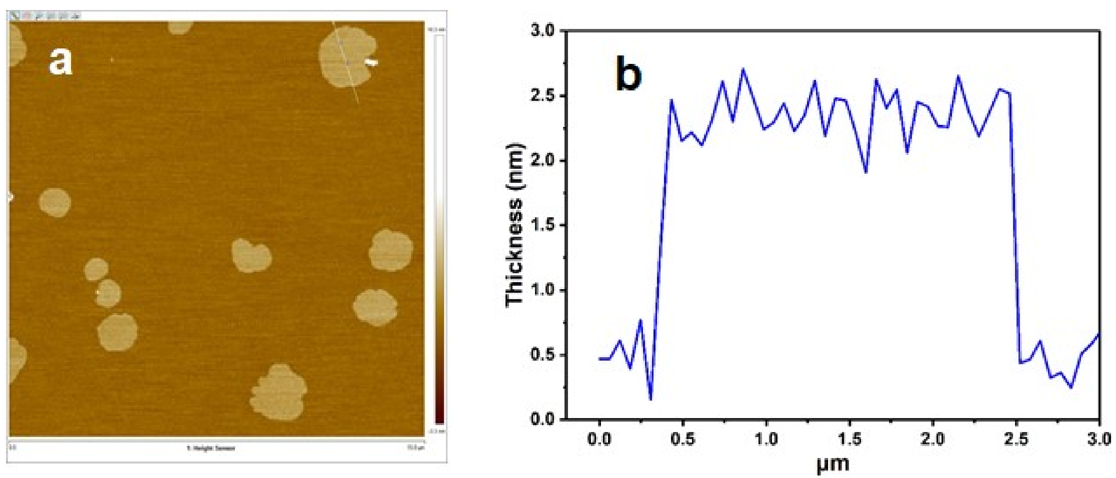

Figure S2. (a) AFM image and (b) the corresponding height measurement of BNNS.

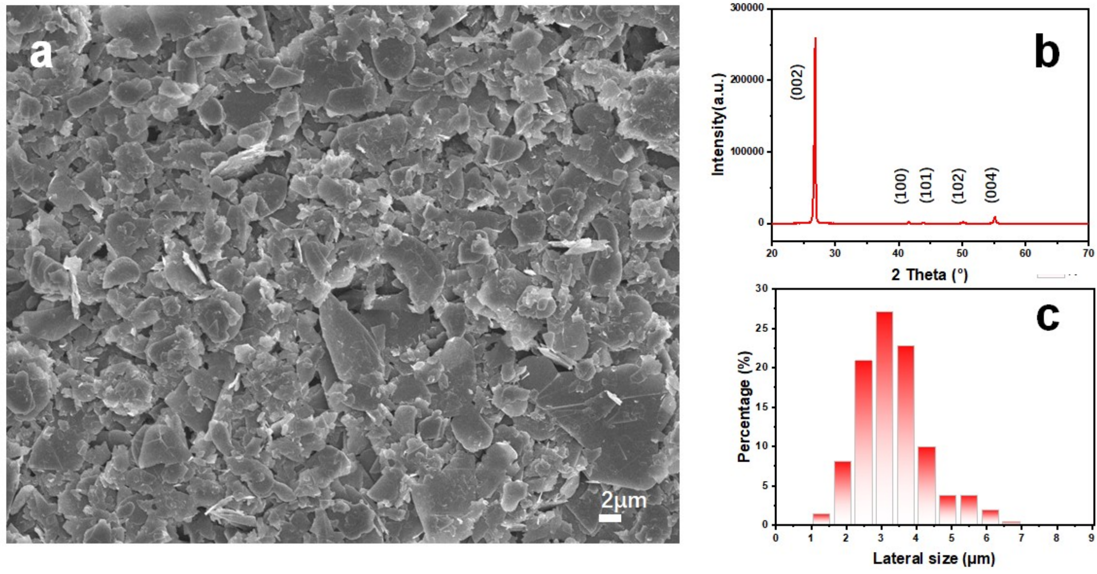

Figure S3. (a) SEM image of the prepared BNNS dispersion. (b) XRD of BNNS. (c) Size distribution of BNNS dispersion.

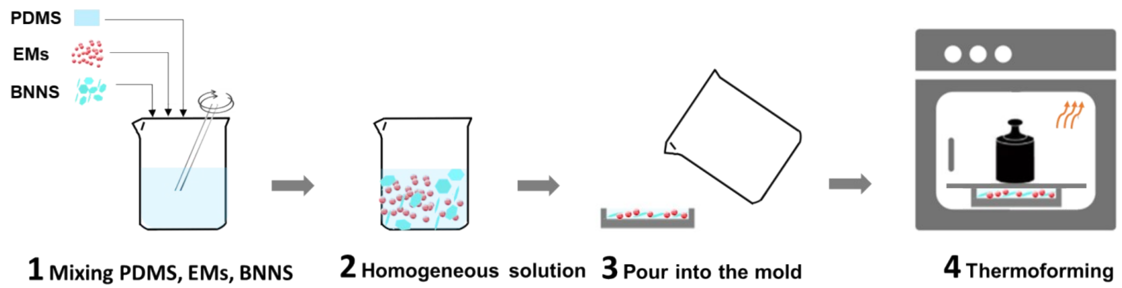

Figure S4. Schematic illustration of the preparation of BNNS/EM/PDMS composites.

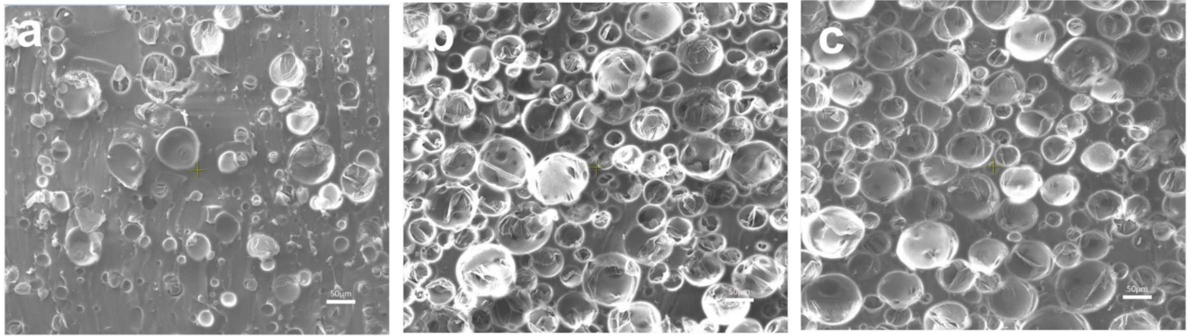

Figure S5. Optimization of inhibitor concentration. SEM images of the EM/PDMS with (a) 1 wt % inhibitor, (b) 3 wt % inhibitor, and (c) 6 wt % inhibitor. 1 wt % inhibitor does not appear to be sufficient to allow full expansion of EMs. Inhibitors with 3 wt % and 6 wt % show similar effect. Therefore, 3 wt % inhibitor is added to prevent the gelation before the expansion of EMs during curing.

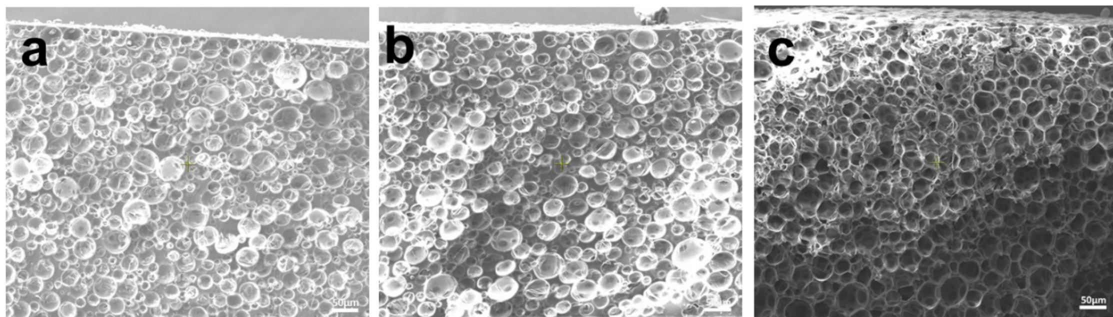

Figure S6. Optimization of EM concentration. SEM images of the EM/PDMS composites with (a) 2 vol% EMs, (b) 3 vol% EMs, and (c) 4 vol% EMs.

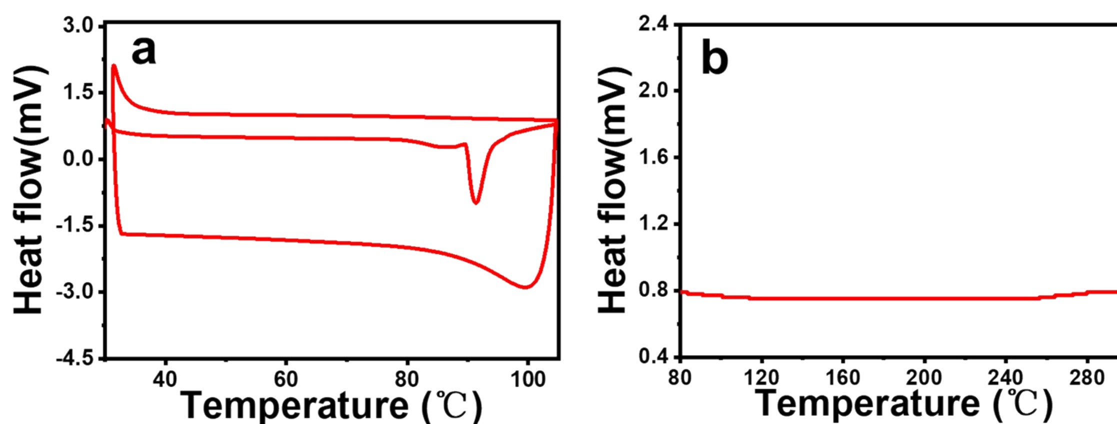

Figure S7. (a) DCS of EMs from 30°C to 105°C for two cycles. The EMs were heated from 30°C to 105°C and then cooled down to 30°C, and heated up again to 105°C. The point 105°C was selected since the EMs expand at ~90°C and start to break beyond 110°C. 105°C ensures full expansion without breakage of the EMs. An endothermic peak shows up at ~ 90°C in DSC, attributed to the vaporization of the liquid core in EMs. If the gas did not escape, an exothermal peak due to the condensation would appear at the cooling stage and the endothermal peak at the same temperature would show up again at the second heating cycle. Neither of the above peaks were observed, indicating that the gas phase in EMs escape during the expansion process. (b) DCS of BNNS/EM/PDMS composite from 80°C to 300°C. No peaks were observed, indicating that the gas phase in EMs escape during the composite's fabrication process.

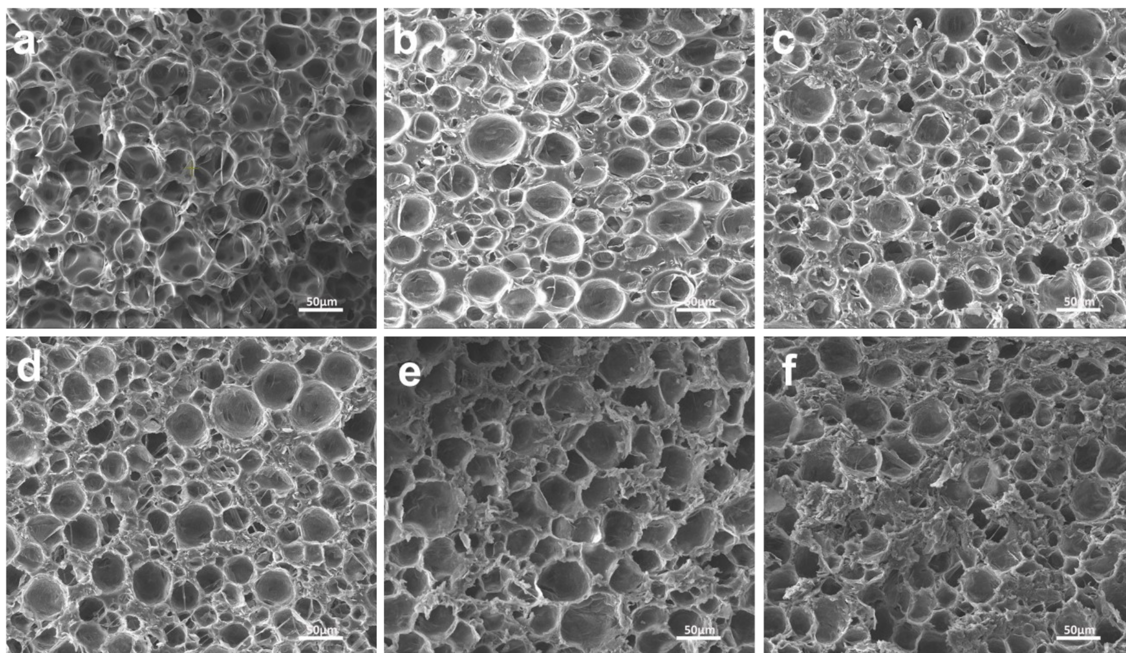

Figure S8. SEM images of BNNS/EM/PDMS composites with different BNNS contents. (a) 0 vol% BNNS, (b) 3.42 vol% BNNS, (c) 4.87 vol% BNNS, (d) 5.86 vol% BNNS, (e) 7.76 vol% BNNS, and (f) 9.82 vol% BNNS.

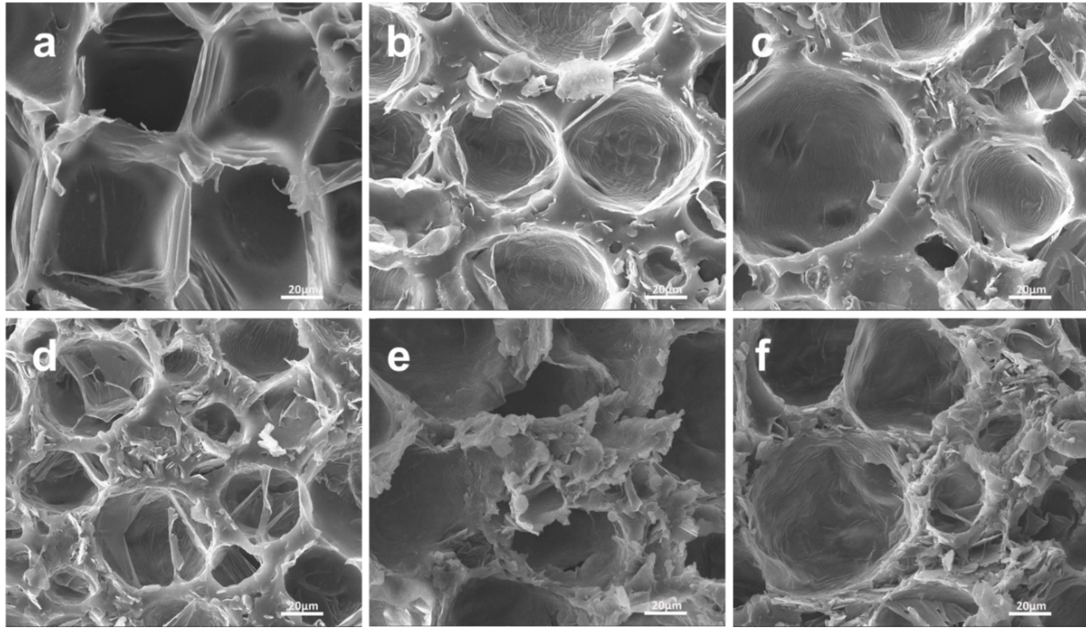

Figure S9. SEM images of composites of different volume percentages at higher magnification. (a) 0 vol% BNNS, (b) 3.42 vol% BNNS, (c) 4.87 vol% BNNS, (d) 5.86 vol% BNNS, (e) 7.76 vol% BNNS, and (f) 9.82 vol% BNNS.

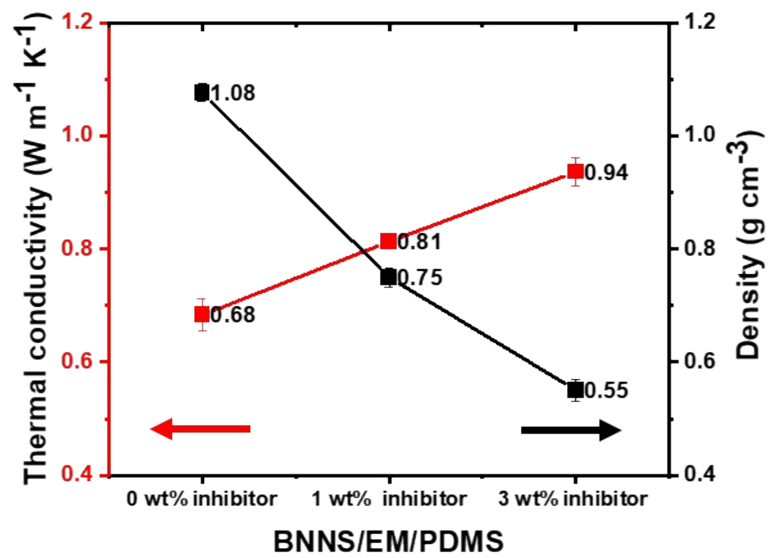

Figure S10. The measured thermal conductivity and density of BNNS/EM/PDMS with different concentration of the curing inhibitor.

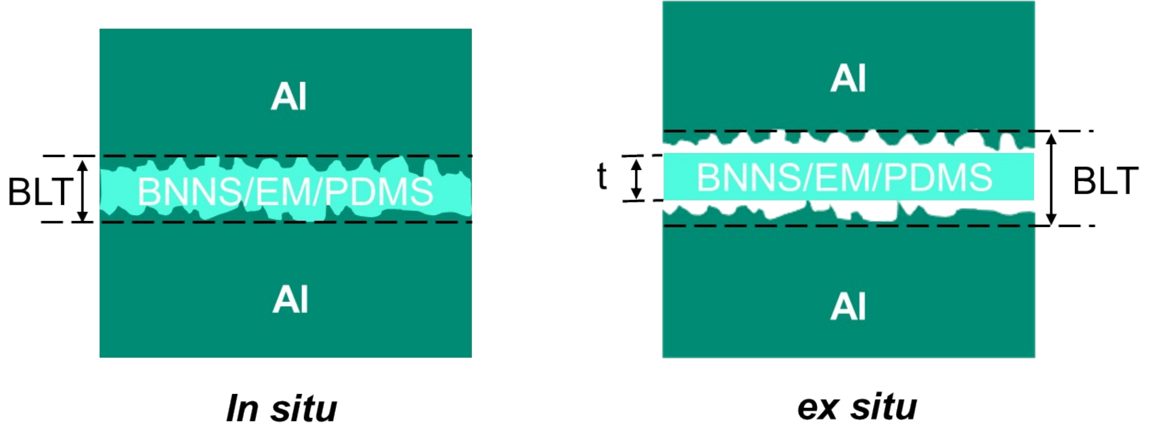

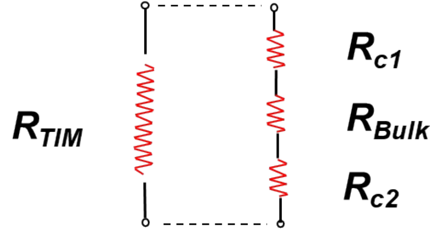

Figure S11. Schematic illustration of thermal contact resistance measurement of *in-situ* and *ex-situ* formed BNNS/EM/PDMS thermal interface material (TIM). Since the thermal resistance of Al plates are negligible, the total thermal resistance (R_{TIM}) is the sum of bulk resistance of the BNNS/EM/PDMS composite (R_{Bulk}) and the contact resistance with the upper and lower Al plates (Rc_1 and Rc_2, respectively), as shown in Equation 1. [1] Detailed parameters are shown in table S1. Note that the bond line thickness (BLT) means the thickness of the TIM under packaging conditions and the thickness of the composite film is denoted as t. For *in-situ* formed sample, $t \approx BLT$, while for *ex-situ* formed sample we assume $t = BLT - 2 \times 0.01$.

$$R_{TIM} = \frac{BLT}{k_{TIM}} = R_{C1} + R_{C2} + R_{Bulk} \qquad (1)$$

Suppose $R_{C1} = R_{C2}$,

$$R_{C1} = R_{C2} = \frac{1}{2}(R_{TIM} - R_{BULK})$$

$$=\frac{1}{2}\left(\frac{BLT}{k_{TIM}}-\frac{t}{k_{Bulk}}\right)$$

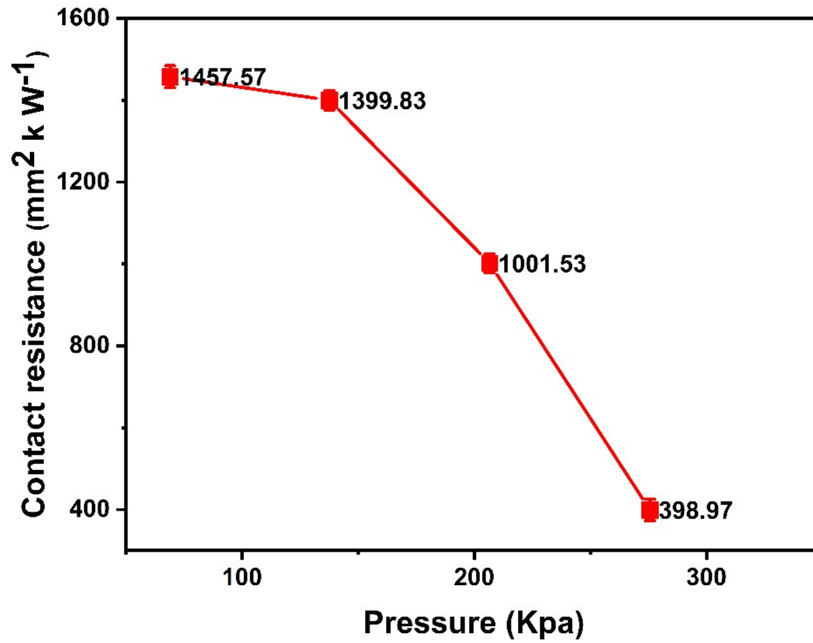

Figure S12. The contact thermal resistance of *ex-situ* formed BNNS/EM/PDMS films under different pressure according to ASTM D5470.

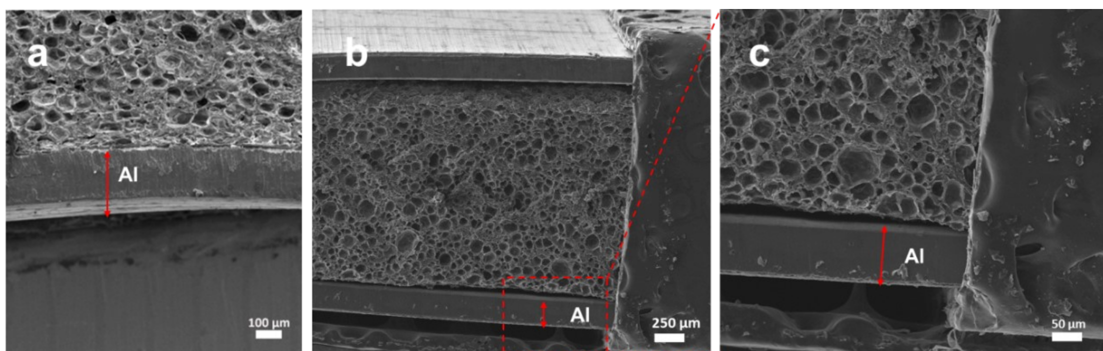

Figure S13. SEM images of (a) the *in-situ* formed BNNS/EM/PDMS composites on Al surface and (b) the *ex-situ* assembled BNNS/EM/PDMS composites between Al surfaces. (c) The magnified image of the gap between composite and Al plate in (b). On the right portion of (b) and (c) is a conductive tape used to press the *ex-situ* formed

composite film on the Al plate. A close contact was not obtained even with the help of the tape.

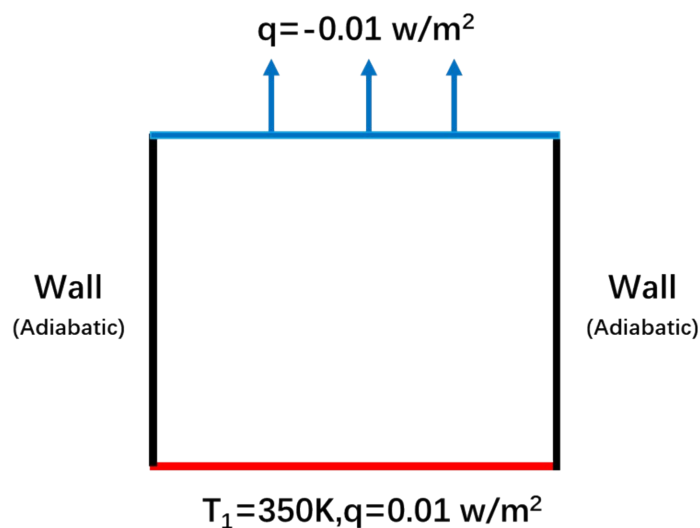

Figure S14. Schematic of the boundary conditions for the simulation model.

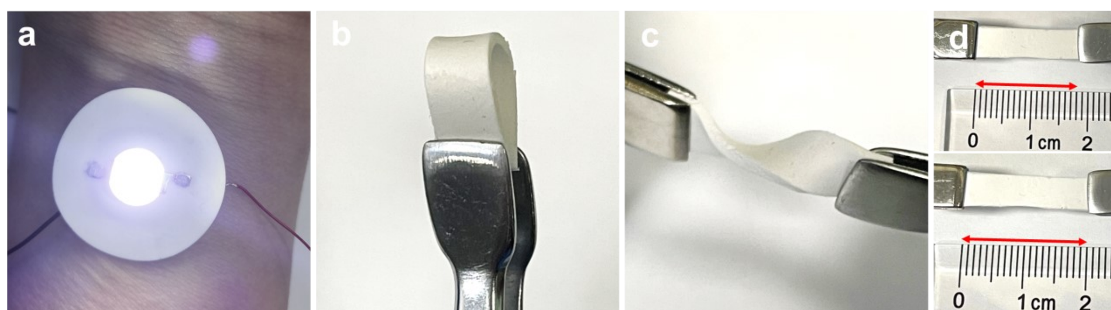

Figure S15. (a) Flexible substrate (BNNS/EM/PDMS) for wearable LED lighting circuits. (b) Bending of the BNNS/EM/PDMS composite substrate. (c) Twisting of the BNNS/EM/PDMS composite substrate. (d) Stretching of the BNNS/EM/PDMS composite substrate up to 10.8% strain.

Table S1. Data list of thermal measurement of Al-BNNS/EM/PDMS-Al sandwiched structure.

Items [units]	BLT [mm]	k_{TIM} [W m^{-1} K^{-1}]	t [mm]	K_{Bulk} [W m^{-1} K^{-1}]	R_{TIM} [W m^{-1} K^{-1}]	R_{Bulk} [W m^{-1} K^{-1}]	Rc_1 [W m^{-1} K^{-1}]
In-situ	1.44	0.915	1.44	0.94	1573.77	1531.91	20.93
Ex-situ	1.46	0.259	1.44	0.94	5637.07	1531.91	2052.58

Table S2. Thermal conductivities of BNNS, EM, and PDMS for the finite element analysis.

Items	k (W m^{-1} K^{-1})
BNNS	600 [2]
EM	0.023 [a)]
PDMS	0.186 [3]

a) As the core of EMs is gas, we use the thermal conductivity of air for EMs' thermal conductivity as an approximation.

References

1 W. Dai, L. Lv, J. Lu, H. Hou, Q. Yan, F. E. Alam, Y. Li, X. Zeng, J. Yu, Q. Wei, X. Xu, J. Wu, N. Jiang, S. Du, R. Sun, J. Xu, C.-P. Wong and C.-T. Lin, *ACS Nano*,2019, **13**,1547-1554.

2 K. Wu, J. Wang, D. Liu, C. Lei, D. Liu, W. Lei and Q. Fu, *Adv. Mater.*, 2020, **32**, 1906939.

3 J. Li, F. Li, X. Zhao, W. Zhang, S. Li, Y. Lu and L. Zhang, *ACS Appl. Electron. Mater.*, 2020, **2**, 1661-1669.